

## Electrical stimulation of human dermal fibroblasts on conducting matrix

© K.A. Kolbe,<sup>1,2</sup> M.A. Shishov,<sup>1,2</sup> I.Yu. Sapurina,<sup>2</sup> N.V. Smirnova,<sup>1,2</sup> V.V. Kodolova-Chukhontseva,<sup>1</sup>  
E.N. Dresvyanina,<sup>1</sup> A.M. Kamalov,<sup>1</sup> V.E. Yudin<sup>1,2</sup>

<sup>1</sup>Peter the Great Saint-Petersburg Polytechnic University,  
195251 St. Petersburg, Russia

<sup>2</sup>Institute of Macromolecular Compounds, Russian Academy of Sciences,  
199004 St. Petersburg, Russia  
e-mail: nvsmirnoff@yandex.ru

Received May 27, 2021

Revised August 10, 2021

Accepted August 11, 2021

Conducting composite based on biocompatible chitosan and single wall carbon nanotubes was used as a matrix for electrical stimulation of human fibroblasts. Parameters of ionic and electronic currents passing through the matrix upon applying cyclic potentials ( $\pm 100$  mV) were studied; the scaffold demonstrated high stability in the course of prolonged electric cycling. It was shown that preliminary electrical stimulation facilitated proliferative activity of human dermal fibroblasts in comparison to that of intact cells.

**Keywords:** chitosan/carbon nanotube composite, electrical stimulation, dermal fibroblasts.

DOI: 10.21883/TP.2022.15.55275.160-21

### Introduction

Electrostimulation techniques are widely used in medicine both for the treatment of a wide range of diseases and for their diagnosis. It has been found that exposure to weak pulse currents increases the activity of the peripheral and central nervous systems, triggering a response in them. This helps to restore musculoskeletal function, stimulate breathing and heartbeat, and treat eye and ear ailments. Electrical stimulation inhibits atrophic and sclerotic changes while stimulating regenerative processes in the circulatory, lymphatic and metabolic systems, which is actively used in regenerative medicine [1].

To optimize electrostimulation protocols, the underlying mechanisms involved in therapeutic approaches are currently being investigated. Such mechanisms include changes in cell behavior in terms of cell proliferative activity, programmed death, differentiation, etc. under the influence of exogenous electrostimulation. Thus, the use of direct current and electrodes with increased capacitive properties has been shown to stimulate the proliferation and growth of bone marrow mesenchymal stem cells, which ensures effective bone tissue repair after fractures. Bipolar electrical stimulation increases the regeneration rate of sensory and motor nerves and has been successfully used in the treatment of human carpal tunnel syndrome [2]. There appears to be unexplored potential for the use of electrostimulation for anti-tumor therapy, treatment of keloid diseases, tissue innervation disorders, skeletal muscle atrophy, etc. [2]. A series of clinical trials *in vivo* and *in vitro* have demonstrated a positive response to electrical stimulation of dermal fibroblasts, leading to improved healing of skin and soft tissue lesions [3].

Currently, regenerative medicine is increasingly using non-invasive treatment and diagnostic methods that require biocompatible, electrically conductive materials that do not traumatize living tissue. Similar materials are also needed in the new biomedical field — cell therapy, where electrostimulation techniques are used to modulate and accelerate the growth of cell cultures used for treatment [4,5]. Biocompatible conductive materials, which have replaced traditional metal electrodes, are generally composites of biocompatible polymer dielectrics and an electrically conductive component. The role of the conductive component is either carbon or an electrically conductive polymer [5–8].

Carbon materials are stable, inert, non-toxic and have a high level of electronic conductivity. Various carbon allotropes are used as conductive components: carbon black, graphene, carbon nanotubes [9]. However, carbon nanotubes are most commonly used because the one-dimensional shape of the particles allows the percolation threshold of conductivity to be significantly reduced and the required conductivity parameters to be obtained with minimal carbon content

One of the best known and most accessible biocompatible materials is chitosan. It is a polysaccharide derived from biomass: shrimp shells, crabs, locusts, etc. Among biocompatible polymers, in terms of production scale and availability, chitosan ranks second after cellulose derivatives [10]. Chitosan is not only biocompatible but also a biodegradable polymer and also has bactericidal properties [11]. Chitosan-based films, which combine excellent mechanical and antibacterial properties, are used for packaging perishable products [15], the polymer is used for antibacterial cleaning of drinking water [13] and the elimination of decomposition products of pharmaceuticals from the organism [14,15].

Composites of chitosan and carbon nanotubes have been obtained by a number of authors [16–19]. Their optical, mechanical and electrically conductive properties [20,21] have been studied. However, the characteristics of each composite are individual. They depend on many factors: the type of carbon nanotubes, the molecular characteristics of chitosan, the mass ratio of the components of their distribution in the composite, etc. Therefore, when obtaining such composites, the primary task is to adapt the material to the specific application.

In the present work, a composite of chitosan with single-walled carbon nanotubes was obtained to study the effect of electrical stimulation on dermal fibroblasts involved in the regeneration of skin and soft tissue injuries. The conditions for obtaining the composite, its composition and properties are summarized. The characteristics of the material when subjected to cyclic potential in both air and physiological solution have been studied. The effect of electrostimulation on the proliferative activity of human dermal fibroblasts by using an electrically conductive composite matrix as a substrate was investigated.

## 1. Materials and methods

### 1.1. Materials

The composite was prepared from 4% aqueous solutions of chitosan (CS) (Biolog Heppe GmbH, Germany,  $M_n = (1.64–2.1) \times 10^5$ ,  $DD = 92\%$ ) and an aqueous suspension of single-walled carbon nanotubes (SWCNT) (Carbon Chg, Russia). The choice of 4.0 wt.% concentration of CS in solution is due to the fact that it has been previously found to be the optimum polymer concentration for coagulation spinning of chitosan fibers [22]. Before preparing the solutions, the aqueous suspension containing SWCNT was dispersed using IL10-0.63 ultrasonic dispersant for 15 min at 25 kHz and power 630 W. The CS powder was added to the resulting aqueous suspension while stirring to achieve swelling and partial dissolution of the CS. Acetic acid was then added to the system to a concentration of 2 wt.% to dissolve the CS completely. After 3 h of stirring the solution was filtered and deaerated in a vacuum chamber for 24 h at 10 kPa. The SWCNT content was 3 wt.% with respect to CS.

CS–SWCNT films were cast by extruding the solution through a slit die onto a glass substrate; casting was followed by drying at 50°C for 1 h. Then, the films on the glass substrate were deaerated in the vacuum chamber for 24 h at pressure of 10 kPa and then dried in air at room temperature for more 24 h. The films were incubated in 10% aqueous solution containing NaOH and  $CC_2H_5OH$  (1:1), for 10 min, then washed with distilled water and air dried [23,24]. The films cast from the obtained solutions were homogeneous and uniformly black.

The conductivity study was carried out under isothermal conditions at  $22 \pm 2^\circ C$  using a four-electrode system. The current source was a Keithley 6487 picoamperimeter source

and a millivoltmeter B7-40/4 was used to record the potential difference.

Mechanical properties were examined using Instron 5943 device, testing base 10 mm, sample tensile speed 10 mm/min. Before tensile testing, the film samples were kept in a desiccator at a relative humidity of 66% for at least 24 h.

### 1.2. Studies *in vitro*

For the studies, a strain of conditionally healthy donor skin fibroblasts obtained from the cell culture collection of the Institute of Cytology of the Russian Academy of Sciences (St. Petersburg) was used. Cells were cultured in complete DMEM medium (Paneco, Russia) supplemented with 1% L-glutamine 200 mM, 10% fetal bovine serum and 1% antibiotics (100 units/ml penicillin, 100  $\mu g/ml$  streptomycin), 1% antimycotic (amphotericin B 250  $\mu g/ml$ ) (all Thermo Fisher Scientific, USA). Cultivation was carried out in a CO<sub>2</sub> incubator (Thermo Fisher Scientific, USA) at 37°C, a CO<sub>2</sub> concentration of 5% and elevated humidity. Cells up to 15 passages were used for the studies.

### 1.3. Electrostimulation equipment

Experiments on electrical stimulation of human dermal fibroblasts on CS–SWCNT electroconductive matrix were performed using Potentiostat/Galvanostat ELINS P-30J instrument, which allows recording currents in the range from 10 nA to 2 A and potentials in the range 80  $\mu V$ –15 V. Possible forms of time sweep of current and potential signals include steady-state, sawtooth,  $\Pi$ -shaped, pulsed and programmable. Maximum logging speed is 1580 points/s.

The cells were electro-stimulated in a specially designed cell made from a single piece of Teflon and without adhesive connections (Fig. 1). A conductive matrix was placed at the bottom of the cell and either electrolyte or culture medium was poured in. The removable electrodes, which were fixed in the grooves of the cell body, were applied to the sample from above. The electrode was a Teflon plate with a platinum wire attached to the end. A potential was applied to the sample through a platinum wire electrode of 1 mm diameter attached to the bottom of the plate. The distance between the parallel electrodes was 9 mm.

### 1.4. Electrostimulation and cell proliferative features research

Electrostimulation was performed on CS–SWCNT films washed repeatedly with physiological solution with neutral pH and sterilized in an autoclave (120°C, 40 min) just before the experiments with the cell material. Sterilization was carried out in an electrostimulation cell where the CS–SWCNT film was placed at the bottom of the bath and sandwiched between two electrodes. Feeding medium with cells was placed in a sterilized cell on top of CS–SWCNT conductive film, the cells were cultured 24 h in a CO<sub>2</sub>

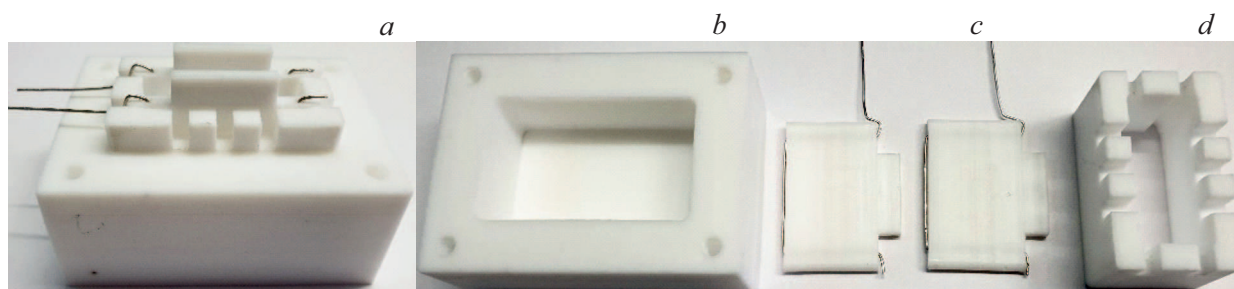


**Figure 1.** *a* — electrostimulation cell assembly and cell components, *b* — bath, *c* — electrodes, *d* — fixing frame.

Mechanical characteristics of the composite films CS–SWCNT

Films	Strength, MPa	Modulus elasticity, GPa	Deformation, %
CS	$124.17 \pm 5.42$	$2.62 \pm 0.57$	$38.68 \pm 4.84$
CS + 3% SWCNT	$158.91 \pm 17.23$	$3.57 \pm 0.26$	$41.16 \pm 5.82$

incubator (Thermo Fisher Scientific, USA) at a temperature of 37°C, CO<sub>2</sub> concentration of 5% and elevated humidity. The duration of electrostimulation was 4 h, during the period of electrostimulation the cell with the cells was in a CO<sub>2</sub> incubator. Using a potentiostat, a cyclic *Pi*-shaped signal was applied to the sample with a polarity reversal every 30 s with an upper and lower potential of +100 and –100 mV, respectively.

Long-term monitoring of cell growth in real time was performed using the RTCA iCELLigence system (ACEA Biosciences, Inc., USA) (Fig. 2, *a*), which allows the analysis of cell culture condition in dynamics by impedance changes. Each well of the E-Plates L8 tablet used in the system contains a set of gold counter-pin electrodes, which allows the resistance created by the cells to be measured (Fig. 2, *b*). Adhesion, spreading and proliferation of cells on the electrode surface increase the resistance of the medium (Fig. 2, *c*) and are recorded as a cellular index: the ratio of impedance at a given time to the initial impedance value. For these studies, cells from the surface of CS–SWCNT matrices that underwent a cycle of electrostimulation, as well as control intact cells, were transferred to the wells of E-Plates L8.

## 2. Results and discussion

The SS–SWCNT films with 3 wt.% carbon content were uniform in thickness (40 μm), and had a deep black coloration, indicating a homogeneous SWCNT distribution. The films had good mechanical properties, the values for strength, modulus of elasticity and deformation of the materials are shown in the table below.

The electrical conductivity of the CS + 3% SWCNT film was isotropic and was  $0.1 \pm 0.005$  S/cm, which is 2 orders of magnitude higher than that of the culture medium ( $0.15 \cdot 10^{-2}$  S/cm), hence, the electric current will preferentially flow over the CS + 3% SWCNT film surface. The electrical conductivity of chitosan films with different SWCNT content was studied in [25], where it was shown that decreasing the SWCNT concentration in the composite film results in current flowing predominantly through the culture medium.

## 3. Electrical properties of CS–SWCNT matrices

A preliminary study of CS–SWCNT matrix samples in both the dry state (22°C and humidity 40–60%) and in electrolyte solution (EP) was carried out in the fabricated cell. The dry matrix exhibits an ohmic volt-ampere relationship in both the positive and negative region of the potentials investigated (Fig. 3). However, when the EP is introduced into the cell and the matrix gets wet, its volt-ampere characteristics dramatically change. The currents are reduced by an order of magnitude and the volt-ampere relationship takes the form of a saturated curve (Fig. 3, inset). This is because the CS–SWCNT composite consists of two conductor types: an electronic type conductor — SWCNT and an ionic conductor — CS [26]. In dry state, ionic conductivity is suppressed, only SWCNT electron transport is observed, forming a percolation grid in the CS matrix. In the electrolyte solution, ionic transport occurs, in which the CS matrix plays a significant role. Chitosan contains ionogenic amino groups, they protonate in an acidic environment and at 100% humidity and temperature 80°C can provide ionic conductivity of the order  $10^{-3}$  S/cm, acceptable for proton conducting membranes [26]. Under physiological conditions (25°C and at the protonation boundary (pH 6–7), the ionic conductivity of the matrix is lower, nevertheless it has a significant influence on the system current. Ion transport creates an electrical double layer at the electrode interface, resulting in a lower effective electrode voltage and a lower current from tens to units μA.

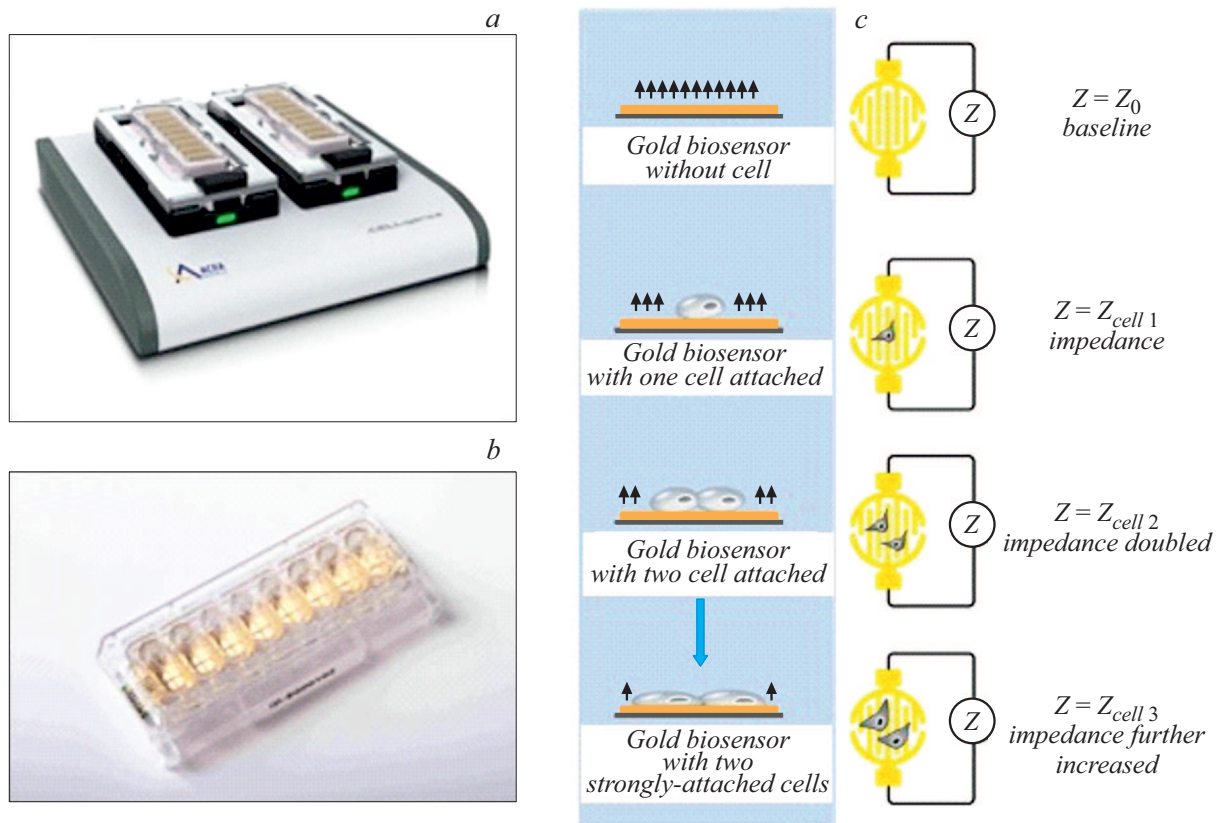


**Figure 2.** *a* — RTCA iCELLigence real-time cell analyzer; *b* — E-Plates L8 electron plate (well spacing is 9 mm from center to the center of adjacent wells according to ANSI standard/SBS 4-2004 for 96-well microtiter tablets); *c* — cell adhesion to the bottom of the electron plate affects the local environment at the biosensor/solution interface, resulting in electrical current impedance ( $Z$ ); impedance varies with cell number and size, the extent of intercellular contacts (cell barrier function) and the efficiency of cell attachment to the substrate.

The contribution of the CS–SWCNT matrix in the formation of the electrical double layer is significantly higher

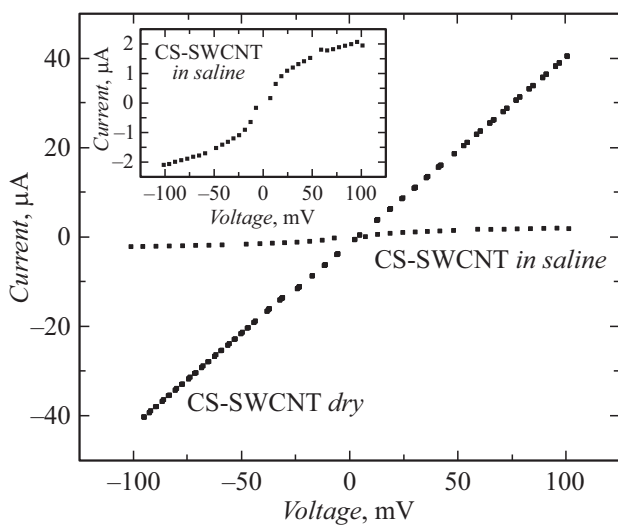


**Figure 3.** Volt-ampere characteristics of CS-SWCNT matrix in dry state and in electrolyte, temperature 25°C, scanning potential rate 3 mV/s, data obtained in an electro-stimulation cell (inset volt-ampere relationship in electrolyte in detail).

than that of the aqueous electrolyte at the border of the electrode, which can be seen by comparing the areas under the curve of the corresponding cyclic voltammety (Fig. 4). Thus, the currents flowing through the stimulated matrix are heterogeneous and complex, not only in terms of the different nature of the carriers, but also in terms of their changing intensity and direction.

#### 4. Electrostimulation of dermal fibroblasts on the surface of the CS–SWCNT matrix

In the electrostimulation process, the CS–SWCNT matrix, immersed in culture medium carrying human dermal fibroblasts on the surface, was given a cyclic Π-shaped signal with polarity reversal every 30 s with upper and lower potential limits +100 and -100 mV respectively. The duration of electrostimulation was 4 h, during which time the cell with the biological material was kept in a CO<sub>2</sub> incubator (Thermo Fisher Scientific, USA) at 37°C, a concentration of CO<sub>2</sub> 5% and elevated humidity. Signal polarity reversal was necessary to reduce the polarization phenomena of the cell electrodes as a result of the formation

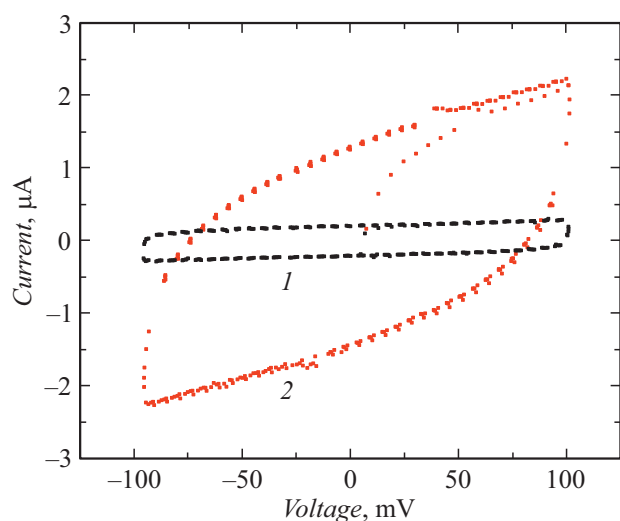


**Figure 4.** Cyclic voltamperograms: 1 — electrolyte; 2 — matrix CS-SWCNT in electrolyte, temperature 25°C, potential scan rate 3 mV/s, data obtained in an electrostimulation cell.

of an electrical double layer at the interface of the solid and liquid phases, and to maintain the average value of the downward current at a level not less than 1  $\mu\text{A}$ .

The shape of the potential applied to the sample and the current flowing through the sample during stimulation, during the first 5 min and at the end, after 4 h of stimulation, are shown in Fig. 5. The current-time plots above show that during continuous 4 h electrostimulation the electrical resistance of the system does not increase, indicating that the CS-SWCNT matrix is stable. The current signal flowing through the sample has a complex shape. When a potential is applied, the current momentarily reaches its maximum value, but then gradually decreases to values close to 1–2  $\mu\text{A}$  due to the electrode polarization.

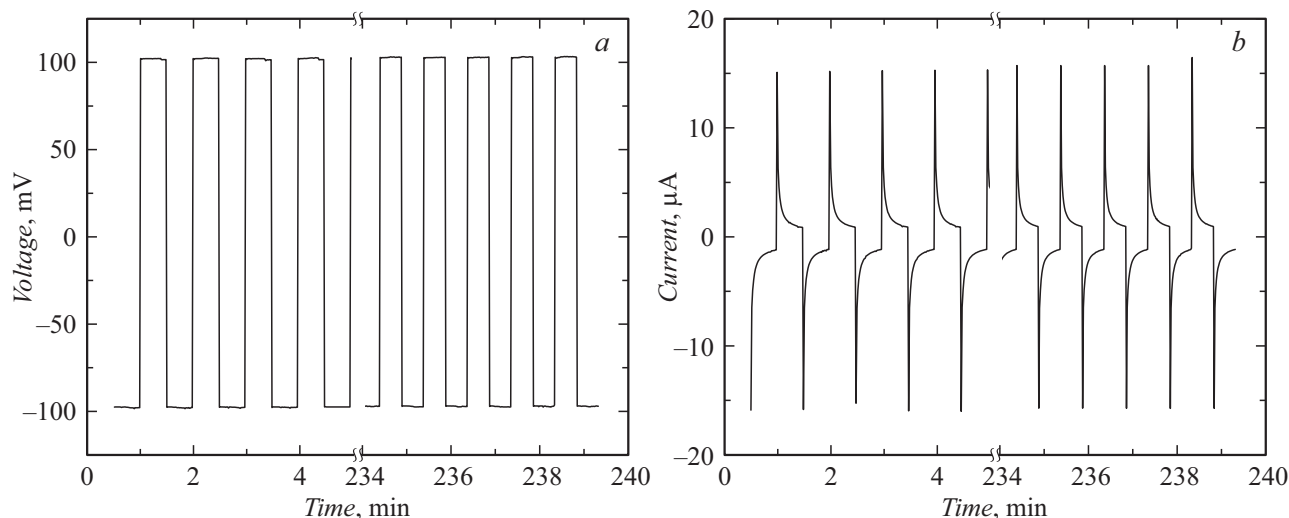


**Figure 5.** Shape (a) of the CS-SWCNT potential (b) current flowing through the sample during the first 5 min and at the end, after 4 h of stimulation. Pulse duration 30 s.

As already discussed, both the culture medium and the CS-SWCNT matrix are ion conductive. The rates of electrostatic equilibrium with the formation of an electrical double layer in aqueous electrolyte solutions correspond to kilohertz frequencies [27]. Thus, under electrostimulation conditions with potential change frequencies on the order of hundredths of a Hz, polarization phenomena with a reduction of the effective electrode potential should occur and lead to a natural reduction of current. Fig. 6 compares the electronic currents observed on the dry CS-SWCNT matrix when a cyclic  $\Pi$ -shaped potential is applied, and the real currents on the CS-SWCNT matrix in culture medium. It can be seen that the real currents alternate according to the change in potential, are symmetrical about the zero potential and have a descending appearance. The average current value on the CS-SWCNT matrix in culture medium is significantly lower than in the CS-SWCNT dry matrix.

## 5. Proliferative features of dermal fibroblast culture after electrostimulation

After electrostimulation, the cells on the CS-SWCNT matrix were multiplied in a 1 pass of cultivation and transferred to a RTCA iCELLigence cell plate, which allows recording of cell culture status dynamically without additional coloring. Cell growth was monitored by changing the impedance created by the cells in a tablet cell fitted with gold electrodes. Adhesion, spreading and proliferation of cells on the electrode surface increase the resistance of the medium and are recorded as a cellular index (CI): the ratio of impedance at a given time to the initial impedance value.

Fig. 7 shows the change over time in CI of dermal fibroblasts subjected to electrostimulation compared to control

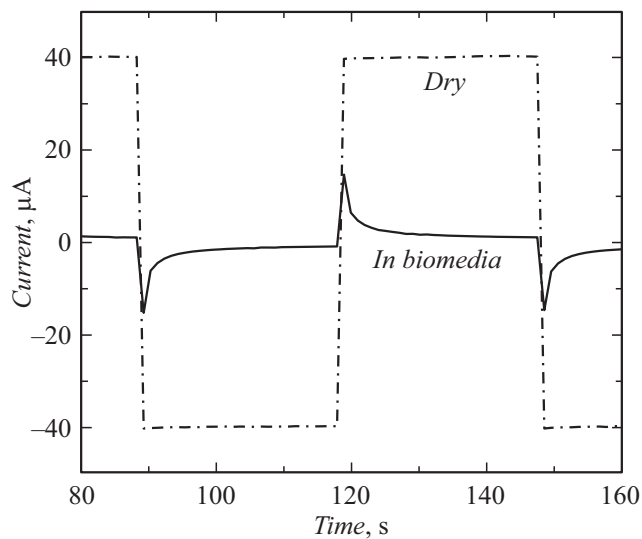


**Figure 6.** Cyclic currents flowing through the dry matrix CS–SWCNT, and through the same sample in culture medium when the electrode potential changes from  $-100$  to  $+100$  mV every 30 s.

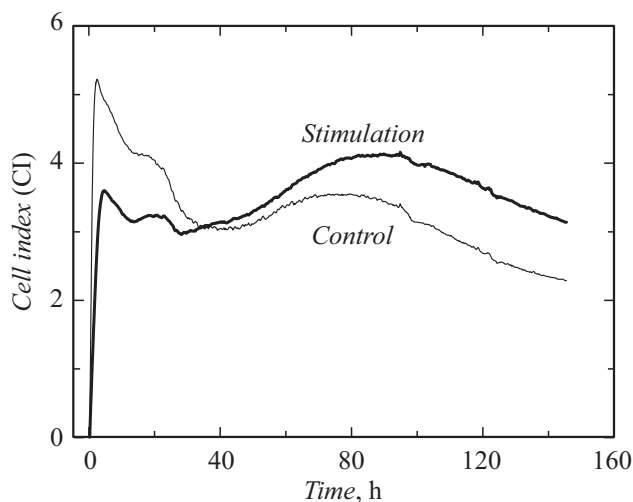


**Figure 7.** Changes in cell index CI during cultivation of human dermal fibroblasts on an RTCA iCELLigence cell assay tablet. Comparison of CI for cells that have and have not undergone pre-stimulation on the CS–SWCNT matrix.

samples without electrostimulation. During the first day, the CI curves of adhesion and unfolding processes in fibroblasts after electrostimulation repeat the control cell trajectories, with lower CI values than in the control. After 24 h of cultivation for both stimulated and control cells, an increase in the CI curve corresponding to proliferative activity is recorded. The growth of electro-stimulated cells is significantly more dynamic than that of control cells, it is more prolonged and results in a higher CI value at the plateau, which corresponds to the formation of a cell monolayer. After monolayer formation, both cell samples show a regular attenuation of cell activity due to contact

inhibition processes common to primary non-cancerous cells.

A number of papers have shown that cells are able to perceive and transform electric fields, but the actual mechanism of these processes is still unclear and the subject of research. The electric field seems to affect the cell indirectly through the plasma membrane or its proteins. This is a likely explanation for the decrease in the number of electro-stimulated cells preliminarily adhered to the surface of the electron tablets. The longer-term effects of electrical stimulation are based on changes in membrane potential through redistribution of charged membrane components and interaction with cell signaling mechanisms during changes in  $\text{Ca}^{2+}$  and ATP [28–30] ion concentrations. These cell signaling cascades may underlie the increased proliferative activity of electro-stimulated dermal fibroblast cultures compared to intact cells.

## Conclusion

A chitosan film composite with a 3% content of single-walled carbon nanotubes with both electronic and ionic conductivity types and high stability under potential cycling has been used for electrical stimulation of human dermal fibroblasts. After electrostimulation, the cells were transferred to an RTCA iCELLigence tablet where cell growth was monitored in real time. It was shown that at the initial stage of cultivation, the adhesion and plating processes of electrostimulated cells are less intense compared to the control. However, after 24 h of cultivation the electro-stimulated cells show more dynamic and rapid growth and outperform the control samples in terms of proliferative activity. In application to regenerative technologies for the restoration of skin and soft tissue integrity, specialized electrostimulation modes using CS–SWCNT-based electrically conductive matrices can be used both for modulation of dermal fibroblast culture activity, applied further in cell therapy, and for local effects on cells within damaged tissues.

## Acknowledgments

The authors would like to thank the Russian Science Foundation for supporting research under Grant № 19-73-30003.

## Funding

The research presented in this paper was funded by Grant № 19-73-30003 from the Russian Science Foundation.

## Conflict of interest

The authors declare that they have no conflict of interest.

## References

- [1] J. Day, J. Newman. *Curr. Orthop. Pract.*, **31** (4), 394 (2020). DOI: 10.1097/BCO.0000000000000889
- [2] M.R. Love, S. Palee, S.C. Chattipakorn, N. Chattipakorn. *J. Cell Physiol.*, **233**, 1860 (2018). <https://doi.org/10.1002/jcp.25975>
- [3] J. Hunckler, A. de Mel, J. Multidiscip. Healthcare, **10**, 179 (2017). <https://doi.org/10.2147/JMDH.S127207>
- [4] R. Feiner, L. Engel, S. Fleischer, M. Malki, I. Gal, A. Shapira, Y. Shacham-Diamand, T. Dvir. *Nat. Rev. Mater.*, **3** (1), 317076 (2018). DOI: 10.1038/nmat4590
- [5] V. Lundin, A. Herland, M. Berggren, E.W.H. Jager, A.I. Teixeira. *PLoS ONE*, **6** (4), e18624 (2011). <https://doi.org/10.1371/journal.pone.0018624>
- [6] E.N. Zare, P. Makvandi, B. Ashtari, F. Rossi, A. Motahari, G. Perale. *J. Med. Chem.*, **63** (1), 1 (2020). DOI: 10.1021/acs.jmedchem.9b00803
- [7] Y. Liu, P. Yin, J. Chen, B. Cui, Ch. Zhang, F.Wu. *Hindawi. Int. J. Polym. Sci.*, **2020**, 5659682 (2020). <https://doi.org/10.1155/2020/5659682>
- [8] I.Yu. Sapurina, V.V. Matrenichev, E.N. Vlasova, M.A. Shishov, E.M. Ivan'kova, I.P. Dobrovolskaya, V.E. Yudin. *Polym. Sci. Ser. B*, **62**, 116 (2020). DOI: 10.1134/S156009042001008X
- [9] M.J. Ahmeda, B.H. Hameedeb, E.H. Hummadic. *Carbohydr. Polym.*, **247**, 116690 (2020). <https://doi.org/10.1016/j.carbpol.2020.116690>
- [10] M. Rayung, M.M. Aung, Sh.Ch. Azhar, L.Ch. Abdullah, M.S. Su'ait, A. Ahmad, S.N.A. Md Jamil. *Materials*, **13** (4), 838 (2020). DOI: 10.3390/ma13040838
- [11] S. Bandara, H. Du, L. Carson, D. Bradford, R. Kommalapati. *J. Nanomater.*, **10** (10), 1903 (2020). DOI: 10.3390/nano10101903
- [15] A.P.A. de Carvalho, C.A. Conte. *Trends Food Sci. Technol.*, **103**, 130 (2020). DOI: 10.1016/j.tifs.2020.07.012
- [13] M.J. Ahmeda, B.H. Hameedeb, E.H. Hummadic. *Carbohydr. Polym.*, **247**, 116690 (2020). <https://doi.org/10.1016/j.carbpol.2020.116690>
- [14] K.S. Soppimath, T.M. Aminabhavi, A.R. Kulkarni, W.E. Rudzinski. *J. Control. Release*, **70** (1–2), 1 (2001).
- [15] L. Zheng, Sh. Wu, L. Tan, H. Tan, B. Yu. *J. Biomater. Appl.*, **31** (3), 379 (2016). DOI: 10.1177/0885328216651183
- [16] G. Lekshmi, S.S. Sana, V.-H. Nguyen, Th.H.Ch. Nguyen, Ch.Ch. Nguyen, Q. Van Le, W. Peng. *Int. J. Mol. Sci.*, **21**, 6440 (2020). DOI: 10.3390/ijms21176440
- [17] J. Venkatesana, BoMi Ryua, P.N. Sudhac, S.-K. Kima. *Int. J. Biol. Macromol.*, **50**, 393 (2012). DOI: 10.1016/j.ijbiomac.2011.12.032
- [18] L. Carson, C.K. Brown, M. Stewart, A. Oki, G. Regisford, Zh. Luo, V.I. Bakhmutov. *Mater. Lett.*, **63**, 617 (2009). DOI: 10.1016/j.matlet.2008.11.060
- [19] S. Pok, F. Vitale, Sh.L. Eichmann, O.M. Benavides, M. Pasquali, J.G. Jacot. *ASC Nano.*, **8** (10), 9822 (2014). DOI: 10.1021/nn503693h
- [20] H.U. Lee, Ch. Park, J.Y. Park. *RSC Adv.*, **6**, 2149 (2016). DOI: 10.1039/c5ra23791b
- [21] O.B. Mergen, E. Arda, G.A. Evingu. *J. Compos. Mater.*, **54** (11), 1497 (2019). DOI: 10.1177/0021998319883916
- [22] E. Dresvyanina, A. Yudenko, E. Maevskaya, V. Yudin, N. Yevlampieva, A. Gubarev, M. Slyusarenko, K. Heppe. *Vlak. Textil.*, **25** (2), 27 (2018).
- [23] N.V. Smirnova, K.A. Kolbe, E.N. Dresvyanina, S.F. Grebennikov, I.P. Dobrovolskaya, V.E. Yudin, Th. Luxbacher, P. Morganti. *Mater.*, **12** (11), 1874 (2019). <https://doi.org/10.3390/ma12111874>
- [24] T.V. Smotrina, E.N. Dresvyanina, S.F. Grebennikov, M.O. Kazakov, T.P. Maslennikova, I.P. Dobrovolskaya, V.E. Yudin. *Polymer*, **7** (2), 28 (2020). <https://doi.org/10.3390/cosmetics7020028>
- [25] K.A. Kolbe, A.M. Kamalov, E.G. Feklistov, N.V. Smirnova, V.V. Kodolova-Chukhontseva, E.N. Dresvyanina, I.P. Dobrovolskaya, G.V. Vaganov, V.E. Yudin. *J. Phys. Conf. Ser.*, **1695**, 012054 (2020). DOI:10.1088/1742-6596/1695/1/012054
- [26] N.A.H. Rosli, K.Sh. Loh, W.Y. Wong, R.M. Yunus, T.Kh. Lee, A. Ahmad, S.T. Chong. *Int. J. Mol. Sci.*, **21** (2), 632 (2020). DOI: 10.3390/ijms21020632
- [27] V.S. Bagotsky. *Fundamentals of Electrochemistry* (Chemistry, M., 1988), p. 400.
- [28] F.X. Hart. In: *The Physiology of Bioelectricity in Development, Tissue Regeneration and Cancer*, ed. by Ch.E. Pullar (CRC Press, 2018), p. 22. ISBN 9781138077836
- [29] I. Titushkin, M. Cho. *Biophys. J.*, **96** (2), 717 (2009). <https://doi.org/10.1016/j.bpj.2008.09.035>
- [30] I.A. Titushkin, V.S. Rao, M.R. Cho. *IEEE Tr. Plasma Sci.*, **32** (4), 1614 (2004). <https://doi.org/10.1109/TPS.2004.832625>